Density Functional Studies of the Hydrolysis of Aluminum (Chloro)Hydroxide in Water with CPMD and COSMO

Jaakko J. Saukkoriipi and Kari Laasonen*

Department of Chemistry, University of Oulu, P.O. Box 3000, Oulu FIN-90014, Finland

Received: May 12, 2008; Revised Manuscript Received: August 13, 2008

Car−Parrinello molecular dynamics (CPMD) and the static density functional method (DFT) with a conductor-like screening model (COSMO) were used to investigate the chemistry of aluminum (chloro)hydroxide in water. With these methods, the stability, reactivity, and acidic nature of the chosen chlorohydrate were able to be determined. Constrained molecular dynamics simulations were used to investigate the binding of chlorine in an aquatic environment. According to the results, aluminum preferred to be 5-fold-coordinated. In addition, the activation energy barriers for the dissociation of chlorine atoms from the original chlorohydrate structure were able to be determined. The actual values for the barriers were 14 ± 3 and 40 ± 5 kJ mol^{-1}. The results also revealed the acidity of the original cationic dimer. DFT with COSMO was used to determine free energy differences for the reactions detected in the molecular dynamic simulations. In conclusion, new results and insight into the aquatic chemistry of the aluminum (chloro)hydroxides are provided.

1. Introduction

Aluminum salts are widely used as water purification chemicals. The most common aluminum compounds used as coagulants are aluminum sulfate and aluminum chloride. The effectiveness of aluminum compounds is mainly based on coagulation and flocculation. In coagulation, the surface charge of negatively charged colloidal impurities is reduced by aluminum cations.[1] In flocculation, these destabilized particles join together and form aggregates.[2] Although the principles of action characterizing how these coagulants work are reasonably well understood, many issues are still unresolved including the complete speciation of aluminum compounds in water and the role of counterions.

The speciation of aluminum in aqueous environments has been under investigation for the past few decades. Most of the works published in this field have concentrated on the reaction paths, kinetics, and structural properties of different aluminum species. Both experimental and computational methods have been used to investigate the speciation. The most commonly used experimental methods in the field are potentiometric titration, ^{27}Al NMR spectroscopy, spectrometric detection, and surface analysis.[3−8] In recent years, electrospray ionization mass spectroscopy (ESI-MS) has also been found to be a useful instrument for investigating aluminum speciation in aqueous environments.[9,10] Compared to the other methods, ESI-MS provides the most diversified view of the aluminum species in water. Combined, these methods have enabled the characterization of large numbers of different aluminum compounds from monomers to polynuclear complexes.[11]

Some computational studies over the years have addressed the solvation of aluminum. These studies are normally divided into two categories, static studies for the structures and energetics and molecular dynamics studies. Martinez et al. studied structures and relative energy differences of different neutral and anionic Al_3O_{1-4} clusters using static density functional methods.[12,13] Gowtham et al. reported similar results in their static studies of anionic and neutral Al_3O_n ($n = 6-8$).[14] In our previous studies, we focused on investigating the structures and energetics of aluminum chlorohydrate and aluminum sulfate dimers, trimers, and tetramers (Al_2 to Al_4) using static density functional methods.[10,15] The molecular formulas for our computations came from the ESI-MS studies of Sarpola et al.[9] Most of the computational works mentioned above have concentrated on the structural properties and energetics of different aluminum clusters. However, static calculations have also been used to study the arrangement of the first- and second-shell water molecules in aluminum complexes, as in the studies of Bock et al.[16]

Hydrolysis of the Al^{3+} cation has also been investigated using Car−Parrinello molecular dynamics (CPMD). Ikeda et al. investigated the hydrolysis of aluminum ions in aqueous $AlCl_3$ solution using the constrained CPMD method.[17] Their simulations consisted of one aluminum ion and three chloride ions separately in solution containing 62 D_2O molecules in neutral, basic, and acidic conditions.[17] Sillanpää et al. used the CPMD method to study the solvation of aluminum hydroxide [$Al(OH)_3 \cdot H_2O$, $Al(OH)_4^-$].[18] Although several articles concerning the solvation of aluminum have been published in recent years, there is one common denominator for these investigations: they concentrate on investigating single aluminum ions in water. However, Pophristic et al. investigated the structure and stability of aluminum chlorohydrate monomer, dimer [$Al_2(OH)_2(H_2O)_8Cl_4$], trimer, and hexamer and Al_{13} polymer using CPMD.[19,20] They used simulated annealing to study the dimer in the gas phase having only H_2O and OH moieties in the coordinating positions and four chlorine atoms around the cluster.[19] The stability of the resulting structure was then explored in an aquatic environment (37 H_2O molecules) in simulations of around 10 ps.[19]

In this study, we have investigated the chemistry of cationic aluminum chlorohydrate in water. The starting structure for the simulations was taken from our previous studies.[15] The chosen structure was also the main complex detected for the dimers in the ESI-MS studies of Sarpola et al.[9] As a structure, it is complex enough to describe the chemistry of aluminum salts in water.

* To whom correspondence should be addressed. Tel.: +358 8 553 1640. Fax: +358 8 553 1603. E-mail: kari.laasonen@oulu.fi.

10.1021/jp804176v CCC: $40.75 © 2008 American Chemical Society
Published on Web 10/04/2008

The primary goal was to investigate the stability of the chosen aluminum (chloro)hydroxide and the binding of chloride ions in aquatic environments. At the same time, we were able to estimate reasons for the anomalies detected in the ESI-MS data. Based on the results of this study, we were able to verify that the electrospray mass spectrometric method overestimates the amount of aluminum complexes in water. Because of the uncertainty in the volume of the aluminum cluster, we performed simulations with two different densities. We used constrained CPMD to reveal energy barriers for chlorine dissociation. In conclusion, we note that this thorough investigation provides new insight into the chemistry of aluminum chlorohydrates in aqueous environments.

2. Computational Details

We investigated the hydrolysis of cationic aluminum (chloro)hydroxide $[Al_2(OH)_3(H_2O)Cl_2]^+$ in a liquid environment using both Car−Parrinello molecular dynamics (CPMD) and static DFT calculations with a conductor-like screening model (COSMO). We focused on studying the hydrolysis reaction introduced in our previous work.[15]

2.1. Static Calculations. We employed the Perdew−Burke−Ernzerhof (PBE) gradient correction approximation[21] with the polarized valence triple-ζ (TZVP) basis set throughout the static part of the study. Static calculations were performed using the Turbomole 5.9 program.[22] The resolution-of-the-identity (RI) approximation was used to accelerate the calculations.[23] The liquid environment was modeled using a conductor-like screening model (COSMO) where water is represented as a dielectric continuum and approximated by a scaled conductor.[24] Most of the parameters employed were default parameters of COSMO.[22,24] Optimized radii for O, H, and Cl atoms exist.[25] The radius for chlorine was 2.0500 Å, that for oxygen was 1.7200 Å, and that for hydrogen was 1.3000 Å. The COSMO radius for aluminum (R_{Al}) was determined to be 1.3287 Å. It was determined as follows: The literature value for the Gibbs free energy of hydration of Al^{3+} ion (298.15 K) is −4619.3 kJ mol^{-1}.[26] The optimized COSMO radius for an aluminum ion was calculated using the equation

$$\Delta E_{Solv}(Al^{3+}) = \Delta E_{COSMO}(Al^{3+},R_{Al}) - \Delta E_{Vacuum}(Al^{3+}) \quad (1)$$

where $\Delta E_{COSMO}(Al^{3+},R_{Al})$ is the COSMO-corrected total energy of the Al^{3+} ion and $\Delta E_{Vacuum}(Al^{3+})$ is the total energy of the Al^{3+} ion in gas phase. It should be noted that the Gibbs free energy of hydration of an Al^{3+} ion was revisited and corrected (∼45 kJ mol^{-1}).[27]

Calculations were carried out as full optimization runs. COSMO calculations were tested and determined to be accurate in describing the trends of hydrolysis reactions of aluminum complexes in our previous study.[15] The dielectric constant for the solvent was chosen to be 78.39, which corresponds to the permittivity of water at 298.15 K.

2.2. Dynamics. The initial starting geometry for the simulations was generated by placing a vacuum-optimized structure of aluminum chlorohydrate in the center of a cubic box with sides of 13.2 Å. The simulation box was then filled with either 62 or 65 water molecules, producing densities of 1.03 and 1.07 g cm^{-3}, respectively. Note that the densities were calculated for the deuterated systems. We used 24 Ry cutoffs for the plane-wave expansion and periodic boundary conditions. The equations of motion were solved using the velocity Verlet algorithm. The fictitious electron mass (μ) was 650 au. Simulations were performed in the canonical ensemble (*NVT*) using the Car−Parrinello molecular dynamics (CPMD) approach.[28] The temperature of the simulations was scaled to 350 K using a chain of Nose−Hoover thermostats[29−32] with a characteristic frequency of 100 cm^{-1}. In the beginning of the simulations (∼1 ps), we used the higher frequency of 1000 cm^{-1} to accelerate the relaxation of the systems. The core electrons were described using Vanderbilt ultrasoft pseudopotentials[33−35] for all atoms in the system. Hydrogen atoms were changed to deuteriums to extend the time step to 0.145 fs. The following atomic masses for the nuclei were used: 2.0 amu for hydrogen, 16.0 amu for oxygen, 27.0 amu for aluminum, and 35.4 amu for chlorine. We used the PBE density functional[36] throughout the simulations, and the total charge of the system was +1. The average simulation time was 32−40 ps.

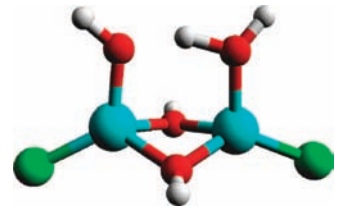

Figure 1. Initial geometry of the simulated aluminum cation $[Al_2(OH)_3(H_2O)Cl_2]^+$. Aluminum is presented in blue, oxygen in red, chlorine in green, and hydrogen in white.

A series of constrained simulations was performed for the system of 65 water molecules. The initial structure of the simulations was taken as a snapshot from a relaxed 65-H_2O simulation in a shell of 13.2 Å sides. The purpose was to investigate the activation energy of dissociation of chlorine atoms from the original aluminum cluster. Energy barriers were calculated separately for one chlorine atom at a time. This was done by fixing the bond length of aluminum and chlorine to a certain value in each simulation and monitoring the constraint force. For each bond length, we carried out an *NVT* simulation of about 15 ps or more to ensure the convergence of the constraint force. We note that only one bond was fixed at a time. The temperature of the simulations was maintained at 350 K using a thermostat with a characteristic frequency of 100 cm^{-1}. The values of the time step, fictitious electron mass (μ), density functional, total charge, and shell were the same as mentioned above. The free energy (activation energy) was then calculated from the equation[37]

$$F = -\int_{r_0}^{r_1} \langle f \rangle_{AlCl} \, dr \quad (2)$$

where F is the free energy of dissociation, r_{AlCl} is the length of the constraint (fixed during each simulation), and $\langle f \rangle$ is the mean force evaluated along the constrained direction.

3. Results and Discussion

3.1. Car−Parrinello Molecular Dynamics. We first focus on the structure and solvation of the aluminum dimer (see Figure 1). The core of this cluster is composed of a ring of two aluminum atoms and two protonated oxygen atoms. In the beginning of the simulation, both aluminum atoms are four-coordinated. Although the structure looks symmetric, it is slightly bent because of different ligands attached to aluminum atoms. The core aluminum−oxygen bond distances vary from 1.84 to 1.88 Å, being shorter on the side of the aluminum bound to the aqua ligand. Determination of the minimum-energy structure for this cationic dimer was described and discussed in detail in our previous studies of aluminum (chloro)hydroxides.[15] None of the previous simulation studies have focused in detail on the stability and solvation of aluminum chlorohydrate

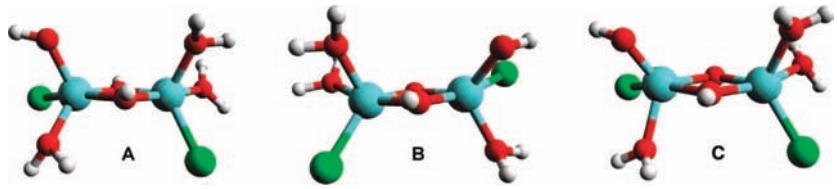

Figure 2. Final geometry of the cluster as determined by (A) 62-H_2O and (B) 65-H_2O system simulations and (C) COSMO optimization.

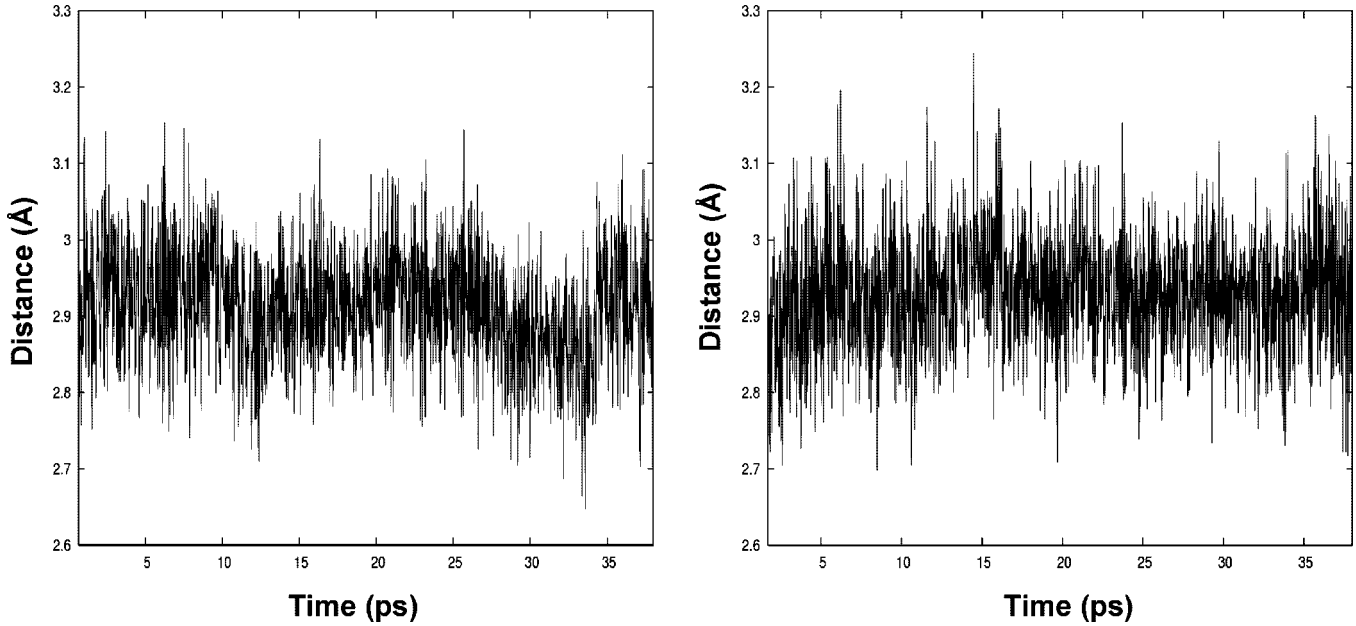

Figure 3. Oscillation of the Al—Al bond distance as a function of simulation time. The 62-H_2O system is on the left, and the 65-H_2O system is on the right.

dimers. Pophristic et al. made one approximately 10 ps simulation in their studies of the $Al_2(OH)_2(H_2O)_8Cl_4$ dimer to check the stability of the cluster in water (37 H_2O molecules).[19] In their studies, both aluminum atoms in the dimer were already six-coordinated in the beginning of the simulation.[19] In this study, we concentrate not only on the stability of the dimer in aquatic environments but also on the hydrolysis reactions of the chosen aluminum chlorohydrate in water. In addition, on the grounds of the results, we are able to improve the prevailing conception of the coordination and acidity of aluminum chlorohydrate dimer in aqueous solutions. Also, for the first time, we are able to provide estimations of the activation energies for chlorine dissociation.

3.1.1. $[Al_2(OH)_3(H_2O)Cl_2]^+$ in Liquid Environments. We performed simulations at two different densities for the cluster in Figure 1. The initial systems contained either 62 or 65 water molecules around the cluster. Simulations were performed for two different initial geometries at both densities. The duration of each of the four independent simulations was 32−40 ps. During this time, we detected significant changes in the primary hydration shell of the cluster (see Figure 2). We used the same notation for the hydration shells as Duan et al.[1] We also note that associative hydration reactions occurred in the first 4 ps. The complete reaction went as follows

$$[Al_2(OH)_3(H_2O)Cl_2]^+ + 2H_2O \rightarrow [Al_2(OH)_3(H_2O)_2Cl_2]^+ + H_2O \rightarrow [Al_2(OH)_3(H_2O)_3Cl_2]^+ \quad (3)$$

During these reactions, the coordination of aluminum increased spontaneously from four to five. Furthermore, the bonding of both of the aluminum atoms changed from tetrahedral to trigonal-bipyramidal. After this reorganization of the cluster, the newly formed aluminum chlorohydrate (Figure 2, structures A and B) stayed intact during the rest of the simulation, which indicates that it is relatively stable in an aquatic environment.

According to previous studies,[19,38] aluminum prefers octahedral coordination in aquatic environments. Therefore, the trigonal-bipyramidal geometry (Figure 2, structures A and B) should still have one spot in the vacant coordination positions in the five-coordinated aluminum atoms to make them ideal for acting as an acceptor of a new donor aqua ligand. However, after the first few picoseconds of the simulations, both aluminum atoms remained shielded, thereby preventing changes in the primary hydration shell. Note that this was true within the time scales (∼35 ps) of the simulations in this study. The Al—Al distance oscillated around 2.95 Å with no visible drift, strengthening our conclusions about the stability of the cluster (see Figure 3). Pophristic et al. reported similar (∼3 Å) Al—Al distances in their CPMD studies.[19]

The Al—O distances varied from 1.80 to 1.93 Å (structure A), being shortest between the aluminum atom and the oxygen atom of the hydroxo ligand. The same was also detected upon analysis of the structural parameters of the structure B. All of the Al—O single-bond lengths detected in this study were within the typical aluminum−oxygen single-bond length range (see Table 1).[39] The hydroxo ligand also had a large effect on the rest of the cluster. The strongly electronegative oxygen attracted valence electrons from the aluminum atom, thereby weakening bonds between aluminum and the other ligands. This can be seen when comparing the two Al—Cl bond distances. The Al—Cl distance on the side of the hydroxo ligand in structure A is approximately 2.33 Å, whereas on the other side, it is about

TABLE 1: Comparison of the Structural Parameters of the Clusters in Figure 2

parameter[a]	bond length (COSMO) (Å) PBE/TZVP	bond length (CPMD[b]) (Å) 62-H_2O PBE	bond length (CPMD[b]) (Å) 65-H_2O PBE
Al—Al	2.94	2.94	2.93
Al*—Cl	2.28	2.33	2.35
Al—Cl	2.18	2.25	2.22
Al*—OH	1.76	1.80	1.79
Al*—OH_2	1.93	1.87	1.88
Al—OH_2 (axial)	1.89	1.85	1.90
Al—OH_2 (equatorial)	1.97	1.92	1.88
Al*—OH (bridge in front)	1.93	1.93	1.92
Al*—OH (bridge in back)	1.88	1.86	1.85
Al—OH (bridge in front)	1.85	1.87	1.86
Al—OH (bridge in back)	1.83	1.85	1.88

[a] Asterisks denote the aluminum atom attached to the hydroxo ligand. [b] Note that CPMD bond lengths are averages taken after every tenth step of the simulations taken from the trajectory file.

2.25 Å (see Table 1). This led to the conclusion that the chlorine attached to the same aluminum atom as the hydroxo ligand is more loosely bound and has a higher tendency to dissociate from the cluster. Furthermore, the two chloro ligands preferred to be orientated on the opposite sides of the structure. More discussion concerning the Al—Cl bonds is provided later in the section on constrained molecular dynamics.

The core of the cluster consisted of one four-membered ring in which the Al—O distances were slightly longer on the side of the hydroxo ligand. This asymmetry in the structure is due to the stronger bond between Al and OH compared to that between Al and OH_2.

Analysis of the structural parameters of structure B shows that most of the bond lengths are similar to those in structure A. The most definite distinction between these structures is the difference in the axial and equatorial Al—OH_2 bond lengths (see Table 1). It should be noted that all of the CPMD bond lengths are averages taken after every tenth step of the simulations taken from the trajectory file. Analyzing structures A and B thoroughly, we can see that, structurally, they are almost identical. This can be confirmed by placing a mirror plane perpendicular to the core of the four-membered ring of structure B so that the plane goes vertically through the hydroxo bridges and projecting the two half-structures on opposite sides. The resulting structure is then identical to structure A. This was confirmed by optimizing both structures with COSMO using the PBE density functional and TZVP as a basis set. The results showed no difference (<0.3 kJ mol^{-1}) in the corrected solvation energies, which strengthened our conclusion about the similarity. In addition, also for structure B, the Al—Al distance oscillated around 2.95 Å without any drift (see Figure 3).

These four independent simulations showed unambiguously that cationic aluminum (chloro)hydroxide dimers prefer at least 5-fold coordination in aquatic environments. In addition, in every case, two different associative hydration reactions occurred during the simulation. From the chemistry point of view, this is interesting because it means that, in the case of aluminum chlorohydrates, most of the low-coordinated aluminum species are unstable in aquatic environments. However, in experimental studies, Sarpola et al.[9] were able to identify several different low-coordinated cationic aluminum dimers. Judging from the results of this study, we were able to show that ESI-MS overestimates the distribution of aluminum compounds in water and that the low-coordinated aluminum species are most probably only artifacts of the ionization conditions of ESI-MS. The electrospray ionization method uses very high voltages,[40] which are used to evaporate the solvent from the sample before it goes into a vacuum for examination. Even though ESI-MS is widely considered to be a mild method for examining ions in solution, it is possible that these high voltages in the solvent evaporation procedure can cause additional fragmentation of the species under investigation. Naturally, simulations have artifacts, such as those arising from the correlation of the outer solvent shells with their own images in CPMD as a result of the small size of the simulation box. However, we feel that this should not be a reason for disagreement with the results because all of the structural changes occurred in the first hydration shell. Furthermore, according to our results, both of the associative hydration reactions occurred on a time scale of picoseconds. The rapidity of the reactions strengthened the conclusion of the instability of low-coordinated complexes in aquatic environments.

3.1.2. Solvation of the Clusters in Both Systems. In this section, we concentrate on the structure of the water surrounding the cluster. This was done by investigating the total HO and OO radial distribution functions. The differences between the total solvation structures of the two systems can be seen in Figure 4. The first peak in the HO RDF at a distance of 0.87−1.16 Å, with a maximum at 0.97 Å, corresponds to the OH distances in water molecules and in the cluster. In the final structure, there were nine different covalent OH bonds, with the rest of the covalent OH bonds belonging to surrounding water molecules. The second peak at a distance of 1.25−2.50 Å corresponds to the acceptor and donor hydrogen bonds in the systems. The maximum of the second peak at around 1.79 Å for both systems is close to the experimental value (1.8 Å) for the hydrogen bond.[41,42] The RDFs g(O,H) and g(O,O) of the two systems are very similar (see Figure 4). This indicates that the total solvation structures in the two systems are almost identical. In addition, the shapes and positions of the peaks in the two RDFs are in good agreement with the water diffraction data of Soper et al.[41,42] In the OO RDF, the first peak at a distance of 2.4−3.3, with a maximum at 2.7 Å, and the second peak at a distance of 3.5−5.4, with a maximum at 4.5 Å, are identical to the experimental values.[41,42] The results are also in very good agreement with the CPMD results of Sillanpää et al.[18] and with the results of liquid water studies by Kuo et al.[43] It is known that the PBE density functional tends to slightly overstructure pair correlation functions.[44,45] In addition, the diffusion coefficient is much smaller than in experiments.[44,45] Slow diffusion should not be a problem in this study because of the relatively high temperature (350 K).

During these simulations, we observed several attempts of the protons of aqua ligands to jump to the surrounding water (see Figure 5). This indicates that the aqua ligands are very acidic. It should be noted that, in all four simulations, the protons stayed attached to the aqua ligands. They diffused only to the secondary hydration shell, and the lifetimes of these hydronium ions were very short (∼1 ps). More information about the existence of hydronium ions in the outer water shells is presented in the next section. The existence of protons as hydronium ions in water agrees well with the studies of Tuckerman et al.[46,47]

The acidity of the aqua ligands was also observed in the analysis of the covalent oxygen−hydrogen bond distance. For the water molecules in the solvent, this distance varied approximately from 0.95 to 1.1 Å with an average of around 1 Å, whereas for the aqua ligands, the distance varied from 0.95 to 1.5 Å, as can be seen in Figure 5. These results provided strong evidence of the acidic nature of the aluminum (chloro)hydroxide clusters.

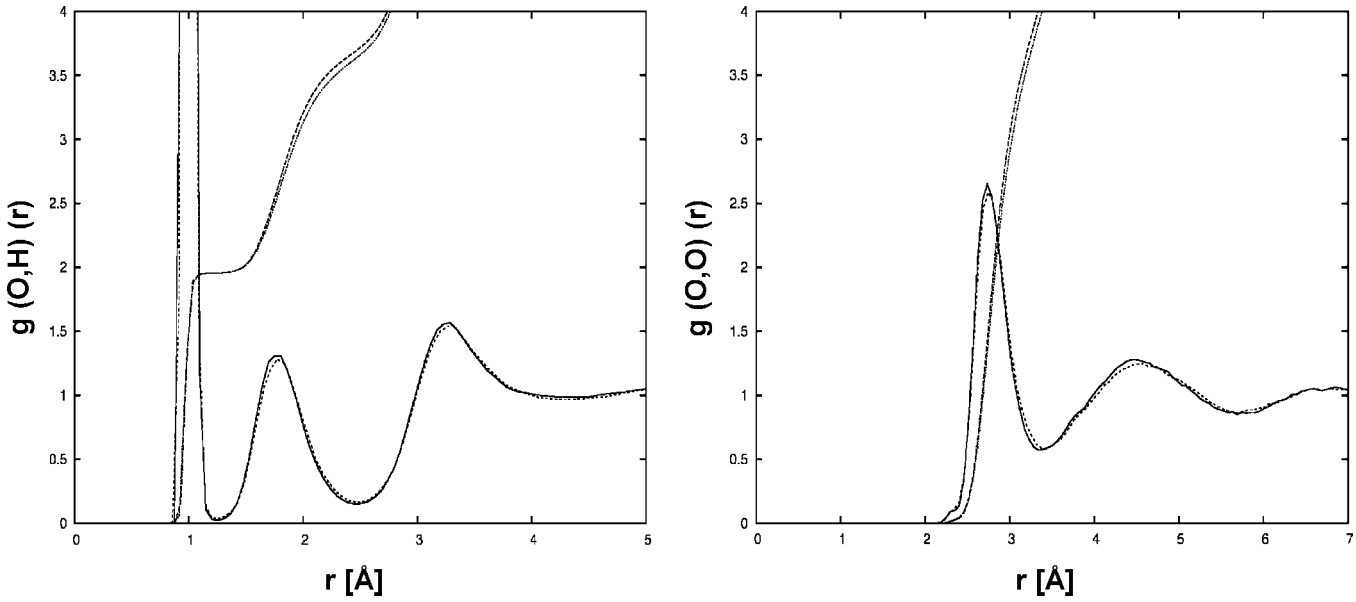

Figure 4. Differences in the total HO and OO RDFs for both the 62-H_2O and 65-H_2O systems. The upper integral (dashed line) and the upper RDF (solid line) are for the denser system (65 H_2O).

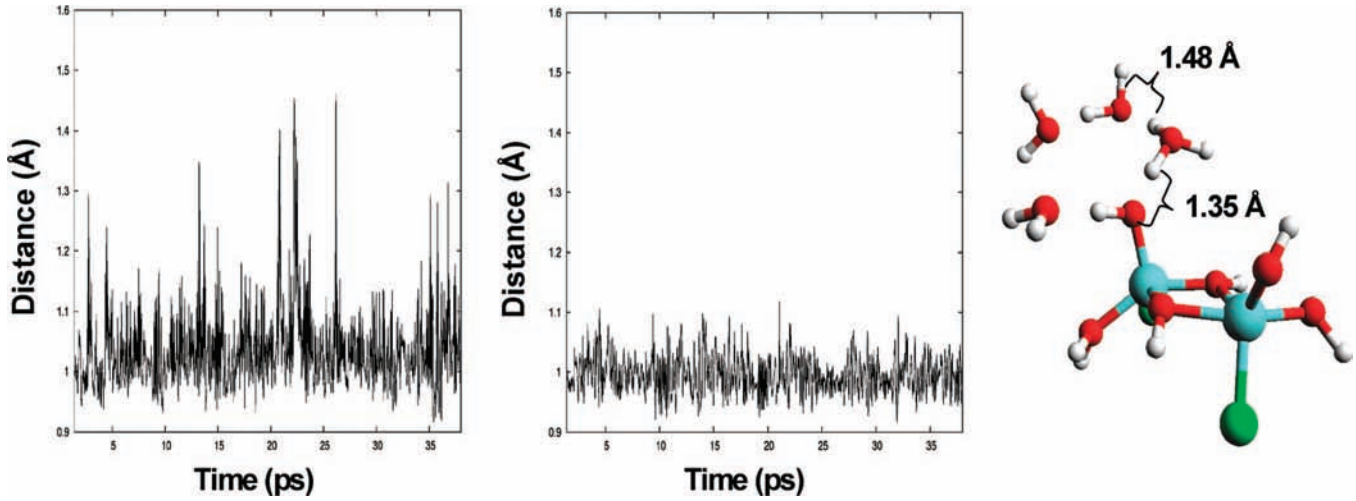

Figure 5. Oscillation of the covalent oxygen hydrogen bond of the aqua ligand (left) and the water molecule of the solvent (center). Spontaneous breaking of one of the aqua ligands (right) leads to the formation of a hydronium ion (H_3O^+) on the secondary hydration shell.

3.1.3. Constraints. The purpose of the constraint calculations was to evaluate the energy barriers for the diffusion of both chloro ligands of the cluster. Simulations were performed with the 65-H_2O system. Constraints were applied by fixing the distance of the aluminum−chlorine bond to a certain value in the actual simulation. In both cases, the constraint force was calculated at nine different points. The length of the simulation depended on the convergence speed of the constraint force. The simulation time was typically around 15 ps. Free energies were then calculated using eq 2.

The average value for the constraint force was calculated using the average of averages. This means that the force was first divided into 10 equal-sized slices of time before averages were calculated. After this, the total average of these 10 individual averages was calculated. Defining the average constraint force was demanding because of large oscillation, as can be seen in Figure 6, which shows a typical example of the raw data of the constraint force. The aluminum chlorine bond length was 2.25 Å, and the force oscillated from −0.02 to 0.01 au. In this case, the average of 10 individual averages was around −0.007 au. We were also able to evaluate the deviation of the force. The range of the variation of averages is shown in Figure 6. The force was then calculated for several different aluminum−chlorine bond distances. Plotting these average forces as a function of bond length, we were able to estimate the actual free energy barriers. The average force was then fitted as a function of distance using a cubic spline. The free energy of dissociation was calculated by integrating the negative area between the two x-axis intersections. The final energy barriers (kJ mol^{-1}) for both of the chloro ligands can be found in Figure 7. The error bars were estimated by fitting the cubic spline for the minimum and maximum values of the constrained force as well.

As expected, the chloro ligand attached to the same aluminum atom as the hydroxo ligand had a much lower dissociation barrier. The free energy for the reaction was 14.0 ± 3.0 kJ mol^{-1}. The magnitude of the barrier indicates that the chloro ligand will easily dissociate to the surrounding water. Nevertheless, spontaneous dissociation did not occur in any of these simulations. We detected only one serious attempt for the spontaneous reaction, but even in this case, the chloride ion bound back to the structure (see Figure 8).

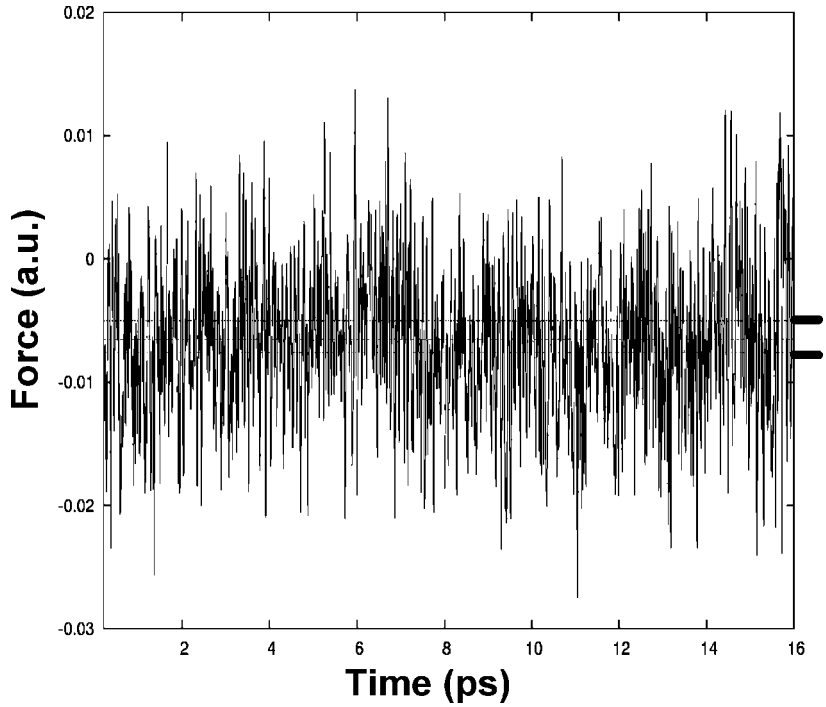

Figure 6. Constrained force as a function of simulation time. Estimation of the dispersion range is shown by the two lines on the right.

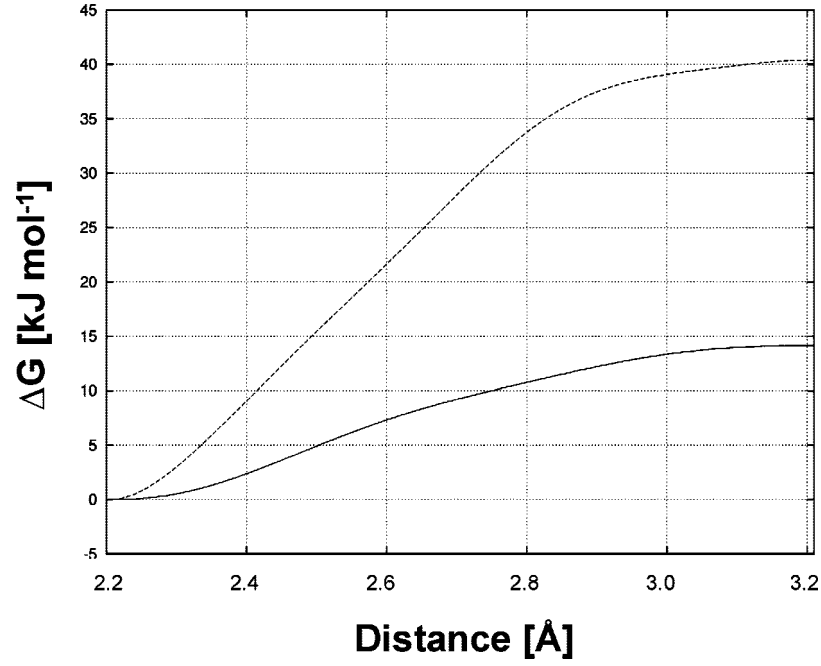

Figure 7. Free energy barriers for the dissociation of both chloro ligands to the surrounding water. The solid line is for the energy barrier of the ligand attached to the same aluminum atom as the hydroxo ligand.

The reaction mechanism for the chlorine escape attempt is interesting because it was induced by a jump of a proton from the oxygen (O**), as can be seen in Figure 8. First, the proton was transferred from the cluster to the water molecule at the distance of 1.68 Å. Because the lifetimes of hydronium ions in the secondary hydration shell were short the proton drifted from the secondary shell to the next water molecule at the distance of 1.65 Å (see Figure 8). The arrow in the figure shows the point in the simulation from which the snapshot is taken. The lifetime of this newly formed hydronium ion was around 3 ps. Even though the chloro ligand was at the greatest distance, over 5 Å from the aluminum atom, it returned to its original position in a little less than 4 ps. This indicates that the chlorine dissociation reaction very likely happens in two phases: First, chlorine has to jump out, and second a water molecule has to replace its position in the cluster. It should also be mentioned that, during this spontaneous reaction, the aluminum−aluminum bond distance also changed at a time of between 30 and 35 ps, as can be seen in the left graph in Figure 3.

We also evaluated the energy barrier for the other chloro ligand. In this case, the free energy for dissociation was 40.0 $\pm$ 5 kJ mol^{-1}. The magnitude of this barrier indicates that this chlorine atom is much more strongly bonded to the aluminum atom than the other chlorine atom. This is due to the weaker electron attraction of the oxygen atom in aqua ligands compared

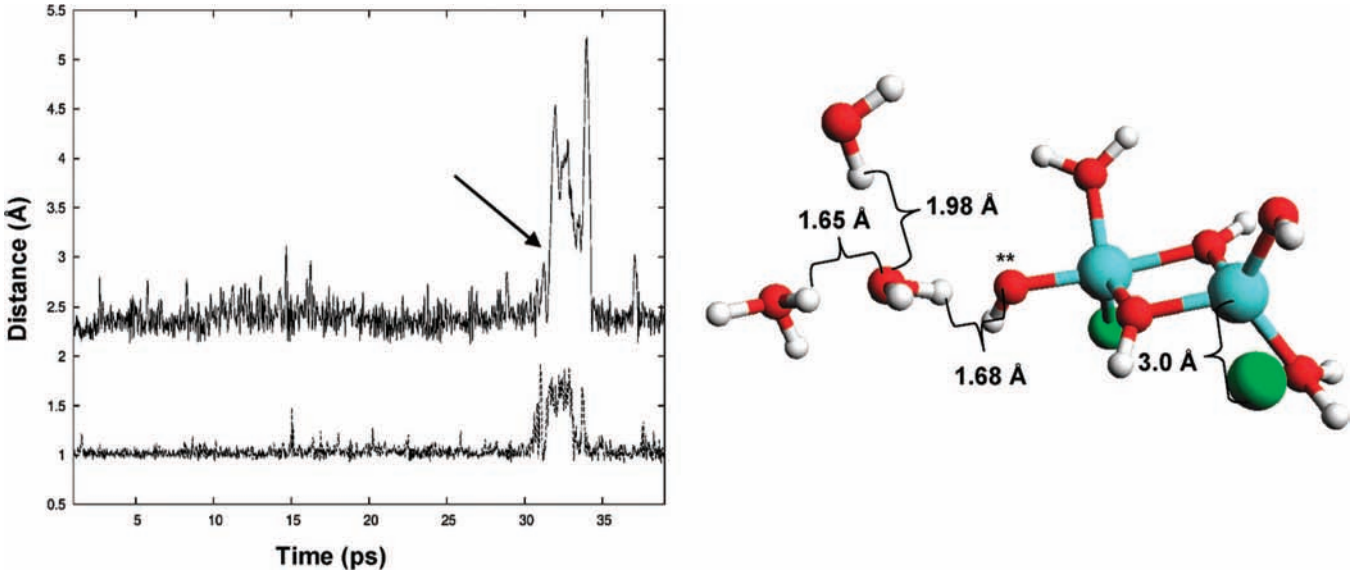

Figure 8. (Left) Al—Cl (upper line) and O**—H (lower line) distances and (right) snapshot of the system in the beginning of the dissociation reaction of the chloro ligand. The arrow points to the position in the simulation from which the snapshot was taken.

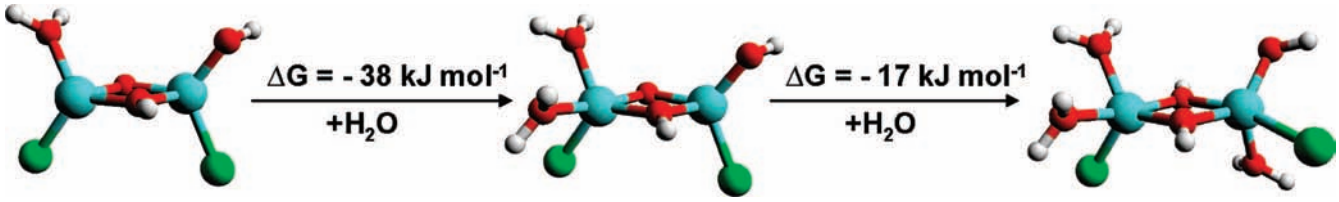

Figure 9. Associative hydration reactions. Free energies for the reactions were calculated using COSMO with PBE density functional and TZVP basis.

to the oxygen atom in hydroxo ligands. Although this was expected, the difference in values was higher than anticipated. On the other hand, it clearly shows the effect of the ligand on the bond dissociation energy barriers. The results show that chlorine atoms are easily dissociated from the aluminum hydroxide structure in aquatic environments, which was already known by experimentalists. This verifies that Car—Parrinello molecular dynamics can be used for predicting and evaluating real-life reactions. We note that constraint simulations were also performed for the 62-H_2O system and the forces were almost identical to the forces calculated in the larger system.

3.2. Associative Hydration Reactions with COSMO. In this section, we compare the results of Car—Parrinello molecular dynamics to those of the conductor-like screening model (COSMO). In the simulations, we detected structural reorganization of the gas-phase optimized cluster. In addition, we observed a series of associative hydration reactions (see Figure 9). The overall reaction occurred as follows: First, the hydration reaction occurred on the aqua ligand side, and second, the hydroxo ligand side was hydrated. The order of these hydration reactions is due to the cone angle. In other words, the stronger and therefore shorter Al—O bond of the hydroxo group produces a larger cone angle, thus shielding the vacant coordination position of the aluminum atom more than the aqua ligand does.

Even though these reactions occurred spontaneously in CPMD, it was very difficult to estimate the free energy differences of the reaction steps. For this purpose, we used static DFT with COSMO. The initial structures for these optimization calculations were taken from the molecular dynamics simulations. The first structure for optimization was a dimer in which both aluminum atoms were four-coordinated. The only difference in relation to the previously optimized gas-phase structure was that the internal hydrogen bond was broken. The free energy differences for these reactions were determined by reducing the solvation energies of reactants from the solvation energy of the product.

The free energy differences show that these reactions are exothermic at room temperature (298.15 K). We note that the solvation energy of the dimers is strongly dependent on the orientation of the chlorine atoms. This was taken into account when performing conformational analysis for all of the complexes. It should be mentioned that stabilizing internal hydrogen bonds were excluded from the analysis so that these results could be compared to the simulations. According to the results of the analysis, chloro ligands preferred trans orientation.

Together, these results indicate that the probability of the existence of low-coordinated aluminum complexes in aquatic environments is very low, at least in the case of aluminum dimers. This finding strengthens the conclusion that most of the low-coordinated complexes are only artifacts of the measuring conditions of the ESI-MS method.

4. Conclusions

We used Car—Parrinello molecular dynamics to investigate the stability, acidity, and reactivity of the chosen aluminum (chloro)hydroxide dimer in aquatic environments. During these simulations, we detected several changes in the primary hydration shell of the cluster. After the first few picoseconds of the simulations, two separate associative hydration reactions were detected. Furthermore, during these reactions, the bonding of aluminum atoms changed from tetrahedral to trigonal-bipyramidal. The complete reaction went as follows: $[Al_2(OH)_3(H_2O)Cl_2]^+ + 2H_2O \rightarrow [Al_2(OH)_3(H_2O)_2Cl_2]^+ + H_2O \rightarrow [Al_2(OH)_3(H_2O)_3Cl_2]^+$.

Constrained molecular dynamics was used to investigate energy barriers of the chloro ligand dissociation reactions. The activation energy for the elimination of the chlorine attached to aluminum on the side of hydroxo ligand was 14 ± 3 kJ mol^{-1}, and that for the chlorine on the other side of the structure was 40 ± 5 kJ mol^{-1}. The magnitudes of these energy barriers reveal that both chlorine atoms are very easily dissociated in aquatic environments.

The independent simulations performed in this study unambiguously showed that aluminum dimers prefer at least 5-fold coordination. In every case, two different associative hydration reactions were detected during simulations. From the chemistry point of view, this indicates that, in the case of aluminum chlorohydrates, most of the low-coordinated aluminum species are unstable in aquatic environments. Furthermore, according to these results, most of the low-coordinated complexes and structural chlorines are most probably only artifacts of the measuring conditions of the ESI-MS method.

A comparison of the results of CPMD and COSMO showed that the two methods complement each other. The reactions mentioned above were verified to be exothermic by the conductor-like screening model. Together, these results revealed that the original gas-phase optimized structure chosen for these investigations was not stable in aquatic environments. Aluminum prefers higher coordination, and chlorine was found to dissociate easily. The large oscillation of the covalent OH bonds of the aqua ligands demonstrated the acidic nature of the aluminum complex. We emphasize that none of the previous computational studies have reported similar results and that the results introduced in this study provided new insight into the chemistry of aluminum (chloro)hydroxide complexes in aqueous environments.

Acknowledgment. The authors thank the Academy of Finland (graduate school, LASKEMO) and the Oulu University Scholarship Foundation for financial support and the Center for Scientific Computing (CSC) for computational resources and expert service. The authors also thank Professor Jürg Hutter for providing a new and enhanced version of the CPMD code and Dr. Ari Seitsonen for useful discussions. Dr. Atte Sillanpää is also acknowledged for general support and useful discussions.

References and Notes

(1) Duan, J.; Gregory, J. *Adv. Colloid Interface Sci.* **2003**, *100*−*102*, 475−502.

(2) Gillberg, L.; Hansen, B.; Karlsson, I.; Nordströmm, E. A.; Pålsson, A. *Water Treatment* **2003**, 115–150.

(3) Baes, C. F.; Mesmer, R. E. *The Hydrolysis of Cations*; John Wiley and Sons: New York, 1976; pp 112−120.

(4) Akitt, J. W.; Greenwood, N. N.; Lester, G. D. *J. Chem. Soc.* **1969**, *A5*, 803–807.

(5) Akitt, J. W.; Greenwood, N. N.; Lester, G. D. *J. Chem. Soc.* **1969**, *D17*, 988–989.

(6) Loring, J. S.; Karlsson, M.; Fawcett, W. R.; Casey, W. H. *Polyhedron* **2001**, *20*, 1983–1994.

(7) Govoreanu, R.; Saveyn, H.; Van der Meeren, P.; Vanrolleghem, P. A. *Water Sci. Technol.* **2004**, *50* (12), 39–46.

(8) Delgado, A. V.; Gonzalez-Caballero, F.; Hunter, R. J.; Koopal, L. K.; Lyklema, J. *Pure Appl. Chem.* **2005**, *77*, 1753–1805.

(9) Sarpola, A.; Hietapelto, V.; Jalonen, J.; Jokela, J.; Laitinen, R.; Rämö, J. *J. Mass Spectrom.* **2004**, *39*, 1209–1218.

(10) Sarpola, A. T.; Saukkoriipi, J. J.; Hietapelto, V. K.; Jalonen, J. E.; Jokela, J. T.; Joensuu, P. H.; Laasonen, K. E.; Rämö, J. H. *Phys. Chem. Chem. Phys.* **2007**, *9*, 377–388.

(11) Casey, W. H. *Chem. Rev.* **2006**, *106*, 1.

(12) Martinez, A.; Tenorio, F. J.; Ortiz, J. V. *J. Phys. Chem. A* **2001**, *105*, 8787–8793.

(13) Martinez, A.; Tenorio, F. J.; Ortiz, J. V. *J. Phys. Chem. A* **2003**, *107*, 2589–2595.

(14) Gowtham, S.; Lau, K. C.; Deshpande, M.; Pandey, R.; Gianotto, A. K.; Groenewold, G. S. *J. Phys. Chem. A* **2004**, *108*, 5081–5090.

(15) Saukkoriipi, J.; Sillanpää, A.; Laasonen, K. *Phys. Chem. Chem. Phys.* **2005**, *7*, 3785–3792.

(16) Bock, C. W.; Markham, G. D.; Katz, A. K.; Glusker, J. P. *Inorg. Chem.* **2003**, *42*, 1538–1548.

(17) Ikeda, T.; Hirata, M.; Kimura, T. J. *Chem. Phys.* **2006**, *124*, 074503.

(18) Sillanpää, A. J.; Päivärinta, J. T.; Hotokka, M. J.; Rosenholm, J. B.; Laasonen, K. E. *J. Phys. Chem. A* **2001**, *105*, 10111–10122.

(19) Pophristic, V.; Holerca, M. N.; Klein, M. L. *J. Phys. Chem. A* **2004**, *108*, 113–120.

(20) Pophristic, V.; Balagurusamy, V. S. K.; Klein, M. L. *Phys. Chem. Chem. Phys.* **2004**, *6*, 919–923.

(21) Ernzerhof, M.; Scuseria, G. E. *J. Chem. Phys.* **1999**, *110*, 5029.

(22) Ahlrichs, R.; Bär, M.; Häser, M.; Horn, H.; Kölmel, C. *Chem. Phys. Lett.* **1989**, *162*, 165–169.

(23) (a) Eichkorn, K.; Treutler, H.; Öhm, H.; Häser, M.; Ahlrichs, R. *Chem. Phys. Lett.* **1995**, *240*, 283–290. (b) Eichkorn, K.; Treutler, O.; Öhm, H.; Häser, M.; Ahlrichs, R. *Chem. Phys. Lett.* **1995**, *242*, 652–660.

(24) Schäfer, A.; Klamt, A.; Sattel, D.; Lohrenz, J. C. W.; Eckert, F. *Phys. Chem. Chem. Phys.* **2000**, *2*, 2187–2193.

(25) Klamt, A.; Schüürmann, G. *J. Chem. Soc., Perkin Trans.* **1993**, *2*, 799.

(26) Burgess J. *Metal Ions in Solution*; John Wiley & Sons: New York, 1978; p 186.

(27) Tissandier, M. D.; Cowen, K. A.; Femg, W. Y.; Gundlach, E.; Cohen, M. H.; Earhart, A. D.; Coe, J. V., Jr. *J. Phys. Chem. A.* **1998**, *102*, 7787–7794.

(28) Parrinello, M.; Hutter, J.; Marx, D.; Focher, P.; Tuckerman, M.; Andreoni, W.; Curioni, A.; Fois, E.; Roetlisberger, U.; Giannozzi, P.; Deutsch, T.; Alavi, A.; Sebastiani, D.; Laio, A.; VandeVondele, J.; Seitsonen, A.; Billeter, S. CPMD; IBM Zurich Research Laboratory and MPI für Festkörperforschung: Zurich, Switzerland, 1995−2001.

(29) Nose, S. *J. Chem. Phys.* **1984**, *81*, 511.

(30) Nose, S. *Mol. Phys.* **1984**, *52*, 255.

(31) Hoover, W. G. *Phys. Rev. A* **1985**, *31*, 1695.

(32) Martyna, G. J. *Phys. Rev. E* **1994**, *50* (4), 3234.

(33) Vanderbilt, D. *Phys. Rev. B* **1990**, *41*, 7892.

(34) Laasonen, K.; Car, R.; Lee, C.; Vanderbilt, D. *Phys. Rev. B* **1991**, *43*, 6796.

(35) Laasonen, K.; Pasquarello, A.; Car, R.; Lee, C.; Vanderbilt, D. *Phys. Rev. B* **1993**, *47*, 10142–10153.

(36) Perdew, J. P.; Berke, K.; Ernzerhof, M. *Phys. Rev. Lett.* **1996**, *77*, 3865.

(37) Trout, B. L.; Parrinello, M. *J. Phys. Chem. B* **1999**, *103*, 7340–7345.

(38) Fratiello, A.; Lee, R. E.; Nishida, V. M.; Schuster, R. E. *J. Chem. Phys.* **1968**, *48*, 3705–3711.

(39) (a) Zaworotko, M. J.; Rogers, R. D.; Atwood, J. L. *Organometallics* **1982**, *1*, 1179–1183. (b) Shreve, A. P.; Mulhaupt, R.; Fultz, W.; Calabrese, J.; Robbins, W.; Ittel, S. D. *Organometallics* **1988**, *7*, 409–416.

(40) Sarpola, A.; Hietapelto, V.; Jalonen, J.; Jokela, J.; Laitinen, R. S. *J. Mass Spectrom.* **2004**, *39*, 423–430.

(41) Soper, A. K.; Bruni, F.; Ricci, M. A. J. *Chem. Phys.* **1997**, *106* (1), 247–254.

(42) Soper, A. K. *J. Phys.: Condens. Matter* **2007**, *19* (33), 335206.

(43) Kuo, I.-F. W.; Mundy, C. J.; McGrath, M. J.; Siepmann, J. I.; VandeVondele, J.; Sprik, M.; Hutter, J.; Chen, B.; Klein, M. L.; Mohamed, F.; Krack, M.; Parrinello, M. *J. Phys. Chem. B* **2004**, *108* (34), 12990–12998.

(44) VandeVondele, J.; Mohamed, F.; Krack, M.; Hutter, J.; Sprik, M.; Parrinello, M. *J. Chem. Phys.* **2005**, *122*, 014515-(1−6)

(45) Lee, H.-S.; Tuckerman, M. E. J. *Chem. Phys.* **2007**, *126*, 164501.

(46) Tuckerman, M. E.; Ungar, P. J.; von Rosenvinge, T.; Klein, M. L. *J. Chem. Phys.* **1996**, *100*, 12878–12887.

(47) Tuckerman, M.; Laasonen, K.; Sprik, M.; Parrinello, M. J. *J. Chem. Phys.* **1995**, *103*, 150–161.

JP804176V